Triple Chain Model of the Reconstructed Mo(001) Surface

Detlef-M. Smilgies,[1,2] Peter J. Eng,[2,3] and I. K. Robinson[2,3]
[1]*Max-Planck-Institut für Strömungsforschung, Göttingen, Germany*
[2]*AT&T Bell Laboratories, Murray Hill, New Jersey 07974*
[3]*Department of Physics, University of Illinois, Urbana, Illinois 61801*
(Received 8 September 1992)

We have studied the high-order commensurate phase of the clean Mo(001) surface at about 100 K with surface x-ray diffraction. Our quantitative structure analysis demonstrates the relevance of the periodic lattice distortion model, but the detailed displacement pattern is closer to a square wave than a sine wave. This probably arises from specific bonding, similar to that seen in W(001).

PACS numbers: 68.35.Rh, 61.10.−i, 68.35.Bs

The discovery that surfaces of certain elements are reconstructed is one of the most exciting revelations of the physics of surfaces. Usually associated with surface phase transitions, the few known reconstructions provide a crucial test of our basic understanding of surfaces. Detailed testing of current theoretical methods can then follow the exact knowledge of the atomic structure. The most striking example of how experimental structural data and theoretical analysis interact can be seen historically in the studies of the (7×7) reconstruction of Si(111) [1,2]. Further examples are seen in recent experimental efforts concentrating on systems involving large unit cells. In some cases these high-order commensurate systems reveal a surprisingly complex ordering of the surface atoms, such as the herringbone ordering of the domains in the reconstruction of Au(111) observed by scanning tunneling microscopy [3] and surface x-ray diffraction [4].

The reconstruction of the clean Mo(001) surface, first discovered with low-energy electron diffraction (LEED) [5], has been studied since with a number of techniques, both experimental and theoretical. Using helium-atom scattering, it was found that the phase transition is driven by a soft surface phonon [6] and that the low-temperature phase is high-order commensurate with a wave vector of $(\frac{3}{7},\frac{3}{7})$ surface reciprocal lattice units (RLU) [7]. The corresponding unit cell has been identified as $c(7\sqrt{2}\times\sqrt{2})R45°$ in a recent LEED investigation [8]. The electronic surface states and the shape of the two-dimensional Fermi surface have been determined as well, through the use of angular-resolved photoemission [9].

Theoretical modeling of this surface phase transition has led to a general understanding that the reconstruction is driven by a delicate interplay of electrons and phonons: The elastic energy required to distort the lattice is overcompensated by a gain in electronic energies associated with the removal of the electronic surface states close to the Fermi level. Agreement has not yet been reached about whether the actual mechanism is due to competing short-range forces [10] or to delocalized interactions [11] such as in a charge-density-wave model. This could be decided by a first-principles approach which now appears to be tractable [12]. An essential test for such a calculation is an accurate experimental determination of the surface structure. Although this has been attempted with high-energy ion scattering [8], we have made the first quantitative diffraction study using the grazing-incidence x-ray technique, known for its very high sensitivity to in-plane atomic positions.

Our experiments were performed at beam line X-16A at the National Synchrotron Light Source, Brookhaven National Laboratory. Dipole magnet radiation was focused with a toroidal mirror and monochromated to an energy of 7.5 keV with a double-crystal Si(111) monochromator. The ultrahigh vacuum (UHV) system, equipped with standard surface diagnostic tools such as a LEED system and an Auger spectrometer, is directly coupled to an x-ray diffractometer specifically designed for surface experiments [13]. The five-circle geometry [14] of this instrument allows us to measure in-plane data as well as out-of-plane scans normal to the surface.

In order to study a well-defined system, the surface has to be prepared in a reproducible fashion. This is particularly difficult in the case of Mo(001), because below 500 K, the surface is highly reactive with respect to hydrogen adsorption. Even small amounts of adsorbed hydrogen result in a different reconstruction [15]. Therefore the surface has to be kept in very good UHV (typically 5×10^{-11} mbar in this study) with a low hydrogen background. Moreover, in order to minimize hydrogen uptake, the surface has to be efficiently cooled, since surface cleaning requires flashing the sample to 2000 K and then cooling down rapidly below the critical temperature of about 170 K. In Fig. 1 we show how the intensity of the $(\frac{11}{7},\frac{11}{7})$ superstructure spot of the clean surface reconstruction and the $(\frac{3}{2},\frac{9}{5})$ spot of the H-induced (5×2) reconstruction [15] develop as a function of time after the flash. The temperature of the sample holder is given in the upper panel. Note that it takes about 50 min before the appearance of the full (5×2)-H structure, that is believed to contain $\frac{1}{10}$ of a monolayer [15]. However, the $(\frac{11}{7},\frac{11}{7})$ intensity is already affected much earlier. In the structural measurements, the total scanning time was divided up into shorter scans of about 1 min duration.

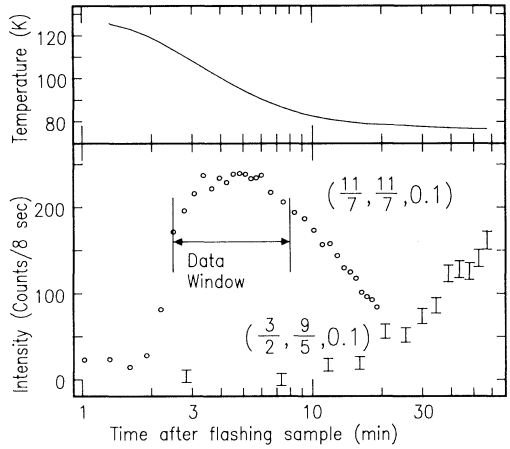

FIG. 1. Time evolution of the $(\frac{11}{7},\frac{11}{7})$ superstructure reflection of the clean Mo(001) surface reconstruction compared with the intensity of the hydrogen-induced $(\frac{3}{2},\frac{9}{5})$ peak. Note the logarithmic time scale. The upper panel displays the temperature of the crystal holder. In the "data window" between 2.5 and 8 min after flashing the sample, the intensity of the $(\frac{11}{7},\frac{11}{7})$ peak and the temperature are almost constant. After such a flash ten scans of a duration of 1 to 1.5 min each were taken. Only scans within the data window were used for the analysis.

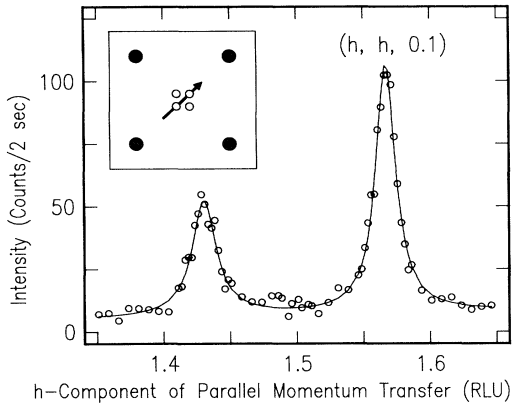

FIG. 2. Scan across two neighboring superstructure reflections of the reconstructed Mo(001) surface. The h component of the parallel momentum transfer is given in reciprocal lattice units (RLU). The scan direction is indicated in the inset showing a schematic LEED pattern (solid circles: 1×1 spots; open circles: superstructure spots). The solid line represents a double-Lorentzian fit. Note the asymmetry in the intensities. This asymmetry was also observed in most of the other zones in the reciprocal lattice.

Only the scans falling within the "data window" indicated in Fig. 1, where the intensity is relatively stable, were averaged together in the final analysis.

Figure 2 shows two of the principal superstructure reflections in a scan along the $\langle 110\rangle$ direction. Although these peaks are the strongest reflections, the peak intensity is only 50 counts/sec. The fitted peak centers are at 10.01 ± 0.04 and 10.97 ± 0.02 times $(\frac{1}{7},\frac{1}{7})$ RLU providing strong evidence for the seventh-order commensurability of this system. Compared with the radial resolution of 0.019 Å^{-1} FWHM, the diffraction peak is somewhat broadened (0.056 Å^{-1} FWHM) indicating an average domain length of about fifty bulk lattice unit cells. This value corresponds roughly to the average terrace length due to the miscut of the sample which was 1.2° and close to the $\langle 100\rangle$ azimuth.

To obtain integrated intensities, transverse scans were measured at a constant grazing incidence angle of 0.4°. We collected 114 superstructure reflections for the first orientational domain. The second domain, rotated by 90°, was found to be weaker in intensity and only the peaks along the diagonal were measured. The fraction of the surface with the second domain was 41%. Both sets of data were merged with appropriate weights and the resulting data set was averaged using $c2mm$ symmetry. The final crystallographic data set consisted of 26 in-plane superstructure reflections and 8 out-of-plane points along the $(\frac{11}{7},\frac{11}{7})$ rod with an overall reproducibility of 15%.

In order to model the data we started with a simple lateral sinusoidal periodic lattice distortion (PLD) [5,16]:

$$\mathbf{R}(i)=\mathbf{R}_0(i)+\mathbf{A}\sin[\mathbf{Q}_s\cdot\mathbf{R}_0(i)]\,.$$

$\mathbf{R}(i)$ and $\mathbf{R}_0(i)$ are the actual and the ideal bulk positions of the surface atoms, respectively, $\mathbf{Q}_s=(\frac{3}{7},\frac{3}{7})$ RLU is the PLD wave vector, and $\mathbf{A}$ is the PLD amplitude, pointing in $\langle 110\rangle$ direction. Applying the $c(7\sqrt{2}\times\sqrt{2})R45°$ symmetry results in an atomic model containing fourteen atoms in the reconstructed unit cell. The amplitude $|\mathbf{A}|$, an overall Debye-Waller factor B, and an arbitrary scale factor were then the only free parameters in a least-squares optimization of calculated versus observed structure factors. A reasonable fit was obtained with a χ^2 of 2.11. The fit value of $A=0.30\pm0.03$ Å differs significantly from the value of 0.20 ± 0.02 Å derived from ion scattering experiments [8] assuming the same model. However, the sinusoidal model fails to explain the intensity difference between the two satellite peaks in Fig. 2 which is seen reproducibly in every zone of the reciprocal lattice (Fig. 3). We therefore allowed the atoms within the unit cell to move independently, subject to the $c2mm$ plane group symmetry constraints, giving three independent displacements in the top layer. An additional displacement for all the atoms in the second layer was also fitted. This fit gave a substantially better χ^2 of 1.36, mainly due to the fact that the intensity asymmetry in the superstructure doublet (Fig. 2) is reproduced. Conversely, if the sign of the displacements was reversed, a substantially worse fit was obtained with the intensity asymmetry inverted. The complete set of structural parameters is displayed in Table I and a comparison between the experimental results and our best model is shown in Fig.

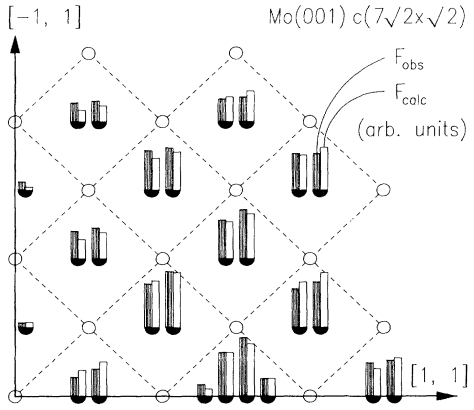

FIG. 3. Comparison between the observed structure factors (left bar) and the structure facture of the best fit model (right bar). The bars are located at the corresponding diffraction spot positions of a single domain. Open circles denote the (1×1) positions, and the solid semicircles underneath each pair of bars, the positions of the $c(7\sqrt{2}\times\sqrt{2})R45°$ superstructure spots.

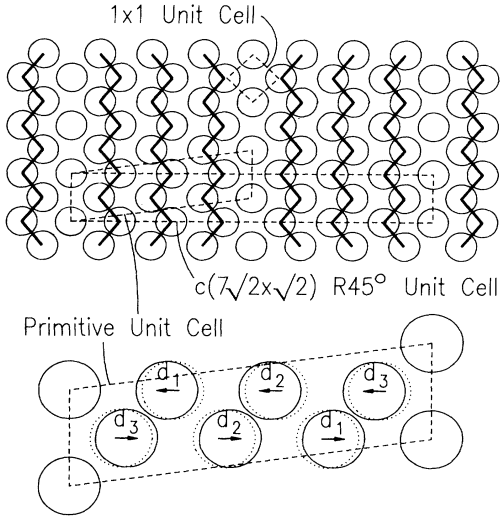

FIG. 4. Structural model for $c(7\sqrt{2}\times\sqrt{2})R45°$ Mo(001). The structure in the regions of displaced surface atoms resembles the well-known structure of the related W(001) surface at low temperatures [17,19]. One out of seven chains on Mo(001) is undisplaced and forms a domain wall between chained regions in antiphase. The (1×1), $c(7\sqrt{2}\times\sqrt{2})R45°$, and the primitive unit cell are indicated by dashed lines. The lower part of the figure shows an enlarged view of the $c(7\sqrt{2}\times\sqrt{2})R45°$ unit cell defining the displacement vectors d_1,d_2,d_3. Atom positions are denoted by solid circles; without the reconstruction the atoms would be in the positions given by the dotted circles. Note that only three independent in-plane displacements are allowed within $c2mm$ symmetry.

3. The out-of-plane data (not shown) did not have much variation, but acted as a constraint on the magnitude of the second layer displacement. Normal components of the displacements were not determined reliably because of the scarcity of out-of-plane data, but an upper limit of 0.5 Å could be estimated before a significant effect on χ^2 was detected.

Our final structural model is shown in Fig. 4. Most of the atoms are strongly displaced and form zigzag chains in the $\langle 110\rangle$ direction as shown. Such behavior is well known for the $(\sqrt{2}\times\sqrt{2})R45°$ reconstructed W(001) surface [17], which is chemically very similar. The interatomic spacings along the different chains are 2.86 ± 0.03 Å and 2.84 ± 0.05 Å, respectively $(4.9\pm1.1)\%$ and $(4.2\pm1.8)\%$ larger than the 2.72 Å nearest-neighbor spacing in the bulk. In W(001) at the surface atoms take part in the chain formation [17] forming the $(\sqrt{2}\times\sqrt{2})R45°$ unit cell, whereas on Mo(001), every seventh row is not displaced, giving rise to the much larger unit cell. This pattern can be viewed as three subunits of the W(001) structure diluted by single-row antiphase domain walls [18]. We therefore refer to this structure as the "triple chain" model. It is noteworthy that the displacements on W(001), 0.24 ± 0.03 Å [19] in the top layer and 0.05 ± 0.02 Å in the second, compare favorably with those in Table I, and the surface bond length along the chain is $(3.8\pm1.1)\%$ longer than the bulk. It is interesting to note that all of the parameters characterizing the W(001) and Mo(001) surface reconstructions agree within the error of their measurement. Indeed, the local similarity of the reconstructions of these two surfaces may be related to the structural and electronic similarities of both systems: Both group-VIB metals have the bcc structure with lattice constants differing by less than 1%.

Even though it was only realized recently that the Mo(001) structure was commensurate, as we have confirmed here, there is a close similarity with models proposed earlier to explain the supposed incommensurate reconstruction. Wang, Tosatti, and Fasolino [20] suggested a soliton model in which order parameter components of M_1 and M_5 symmetry oscillated in quadrature along the $\langle 110\rangle$ direction. Heine and Shaw [21] showed how boundaries between M_1 and M_5 regions could be stabilized by strain relief. These features appear in our model in Fig. 4, except that each antiphase region is exactly three chains long and not incommensurate. Because of the PLD squaring, the soliton or domain wall is a sin-

TABLE I. Final best fit parameters for Mo(001) $c(7\sqrt{2}\times\sqrt{2})R45°$. The parameters are defined in Fig. 4, except for v, the second layer displacement of twelve atoms (all atoms except those on mirror planes), and $B=8\pi^2\langle u^2\rangle$, the overall Debye-Waller factor.

d_1 (Å)	d_2 (Å)	d_3 (Å)	v (Å)	B (Å^2)
0.225(36)	0.231(39)	0.206(28)	0.018(7)	1.4(4)

gle atomic row wide; the displacement d_3 of the row adjacent to the wall is only slightly less than d_1 or d_2. Relaxations within the domains are consequently small, too: The average spacing between the chain center is not significantly (0.01 ± 0.04 Å) larger than an ideal $(\sqrt{2} \times \sqrt{2})R45°$ arrangement.

The displacement magnitudes we show in Table I and the values derived from a previous ion scattering study by Hildner *et al.* [8] show some discrepancy. In their work a smaller displacement amplitude of 0.12 ± 0.02 Å is reported using a similar antiphase domain model. Unlike our work, however, the latter study could not distinguish between the sinusoidal PLD and the antiphase domain displacement models. It is interesting to note that an ion scattering investigation of W(001) [22] also suggested a smaller displacement (0.10 to 0.18 Å) than derived from both LEED [23] and x-ray diffraction [19] analysis (0.24 Å). A possible explanation is the compounding effect of the displacements in the second layer that would effectively "bend" the channels seen by the ions near the surface and thus make the displacements in the top layer appear smaller.

In this work we have given an accurate determination of the high-order commensurate $c(7\sqrt{2} \times \sqrt{2})R45°$ structure of the reconstructed Mo(001) surface at about 100 K. The structure deviates strongly from the simple sinusoidal modulation that is expected close to the critical temperature of 170 K based on the observation of a soft surface phonon [6,7]. Furthermore, we have shown the relationship between the $(\sqrt{2} \times \sqrt{2})R45°$ reconstruction of W(001) and the more complex reconstruction of Mo(001). Locally, they both form zigzag chains of surface atoms which are displaced, to have six nearest neighbors instead of four. The new surface bond length is 4% greater than the bulk in both cases. The difference between Mo and W is that after every three chains on Mo(001) there follows a row of undisplaced atoms that forms an antiphase domain wall between neighboring chained regions. We propose that this difference in behavior is linked to subtle differences in electron-phonon coupling between W and Mo, and therefore suggest that Mo(001) would make an interesting subject for a future total-energy theoretical calculation.

D.M.S. acknowledges a fellowship from the Max-Planck-Gesellschaft, Germany. We thank R. T. Clay for his valuable assistance in data reduction and analysis. The crystal was kindly provided by the Max-Planck-Institut für Strömungsforschung. Göttingen, Germany. NSLS is supported by the Department of Energy under Grant No. DE-AC012-76CH00016. Partial support also came from the University of Illinois Materials Research Laboratory under Grant No. DEFG02-91ER45439.

[1] K. Takanayagi *et al.*, Surf. Sci. **164**, 367 (1985); I. K. Robinson *et al.*, Phys. Rev. B **37**, 4325 (1988).
[2] I. Stich *et al.*, Phys. Rev. Lett. **68**, 1351 (1992); K. D. Brommer *et al.*, Phys. Rev. Lett. **68**, 1355 (1992).
[3] J. V. Barth *et al.*, Phys. Rev. B **42**, 9307 (1990).
[4] K. G. Huang *et al.*, Phys. Rev. Lett. **65**, 3313 (1990).
[5] T. E. Felter, R. A. Barker, and P. J. Estrup, Phys. Rev. Lett. **38**, 1138 (1977).
[6] E. Hulpke and D.-M. Smilgies, Phys. Rev. B **40**, 1338 (1989).
[7] E. Hulpke and D.-M. Smilgies, Phys. Rev. B **43**, 1260 (1991).
[8] M. L. Hildner, R. S. Daley, T. E. Felter, and P. J. Estrup, J. Vac. Sci. Technol. A **9**, 1604 (1991).
[9] K. E. Smith and S. D. Kevan, Phys. Rev. B **43**, 3986 (1991).
[10] I. Terakura, K. Terakura, and N. Hamada, Surf. Sci. **103**, 103 (1981); **111**, 479 (1981).
[11] X. W. Wang, C. T. Chan, K.-M. Ho, and W. Weber, Phys. Rev. Lett. **60**, 2066 (1988).
[12] K.-M. Ho (private communication).
[13] P. H. Fuoss and I. K. Robinson, Nucl. Instrum. Methods Phys. Res., Sect. A **222**, 164 (1984).
[14] E. Vileg *et al.*, J. Appl. Cryst. **20**, 330 (1987).
[15] J. A. Prybyla *et al.*, Phys. Rev. Lett. **58**, 1877 (1987).
[16] R. A. Barker, S. Semancik, and P. J. Estrup, Surf. Sci. **94**, L162 (1980).
[17] M. K. Debe and D. A. King, Phys. Rev. Lett. **39**, 708 (1977).
[18] T. E. Felter, R. S. Daley, M. L. Hildner, and P. J. Estrup, Bull. Am. Phys. Soc. **37**, 273 (1992); (private communications).
[19] M. S. Altman, P. J. Estrup, and I. K. Robinson, Phys. Rev. B **38**, 5211 (1988).
[20] C. Z. Wang, E. Tosatti, and A. Fasolino, Phys. Rev. Lett. **60**, 2661 (1988).
[21] V. Heine and J. J. A. Shaw, Surf. Sci. **193**, 153 (1988).
[22] I. Stensgaard, K. G. Pucell, and D. A. King, Phys. Rev. B **39**, 897 (1989).
[23] H. Landskron *et al.*, J. Phys. Condens. Matter **1**, 1 (1989).